References

Belegundu, A., and Zhang, S., 1992, "Robustness of Design through Minimum Sensitivity," ASME JOURNAL OF MECHANICAL DESIGN, Vol. 114 No. 2, pp. 213–217.

Feng, C.-X., and Kusiak, A., 1994, "Design of Tolerances for Quality," *Design Theory and Methodology,* T. Hight and F. Mistree, eds., DE-Vol. 68, ASME, New York, pp. 19–28.

Kusiak, A., and Feng, C.-X., 1995, "Deterministic Tolerance Synthesis: A Comparative Case Study," *Computer-Aided Design,* Vol. 27, No. 10, pp. 759–768.

Montgomery, D., 1991, *Design and Analysis of Experiments,* Third Edition, John Wiley, New York.

Ostwald, P., and Huang, J., 1977, "A Method for Optimal Tolerance Selection," ASME JOURNAL OF ENGINEERING FOR INDUSTRY, Vol. 109, No. 4, pp. 558–565.

Parkinson, A., Sorensen, C., and Pourhassan, N., 1993, "A General Approach for Robust Optimal Design," ASME *Journal of Mechanical Design,* Vol. 115, No. 1, pp. 74–80.

Parkinson, D., 1993, "Quality-Based Design by Probability Optimization," *Quality and Reliability Engineering International,* Vol. 9, No. 1, pp. 29–37.

Peat, A., 1968, *Cost Reduction Charts for Designers and Production Engineers,* The Machinery Publishing Company Ltd., Brighton, England.

Shingo, S., 1988, *Non-Stock Production Systems: The Shingo System for Continuous Improvement,* Productivity Press, Cambridge, MA.

Womack, J., Jones, D., and Roos, D., 1991, *The Machine that Changed the World: The Story of Lean Production,* HarperCollins, New York.

Zhang, H., and Huq, M., 1992, "Tolerance Techniques: The State-of-the-Art," *International Journal of Production Research,* Vol. 30, No. 9, pp. 2111–2135.

Heat Transfer in the Non-reacting Zone of a Cement Rotary Kiln

P. S. Ghoshdastidar[1] and V. K. Anandan Unni[2]

This paper presents a steady-state heat transfer model for a rotary kiln used for drying and preheating of wet solids with application to the non-reacting zone of a cement rotary kiln. A detailed parametric study indicates that the influence of the controlling parameters such as percent water content (with respect to dry solids), solids flow rate, gas flow rate, kiln inclination angle and the rotational speed of the kiln on the axial solids and gas temperature profiles and the total predicted kiln length is appreciable.

Nomenclature

A = area
E_b = black body emission per unit area
F_{ij} or F_{gj} = shape factor between surfaces i and j (including $j = i$) or between gas and surface j
q = heat transfer
$\dot{m}$ = mass flow rate
N = number of surface elements on the wall and the solid
T = temperature
Δz = size of each axial segment of the kiln

Greek Letters

α = fill-angle
ϵ = emissivity
σ = Stefan-Boltzmann constant, 5.67×10^{-8} $W/m^2 - K^4$
θ = as defined in Fig. 1(a)
τ_g = transmissivity of the gas

Subscripts

g = Gas
i = element number of the wall or the solid
j = element number of the wall or the solid
s = solid
v = vapor
$s, z + \Delta z$ or $g, z + \Delta z$ = first subscript: solid or gas, second subscript: at a distance $z + \Delta z$ from the kiln inlet

1 Introduction

A rotary kiln employed for drying and preheating of wet solids consists of a refractory lined cylindrical shell mounted at a slight incline from the horizontal plane. The kiln is very slowly rotated about its longitudinal axis. The wet solids are fed into the upper end of the cylinder and during the process are dried and heated by the countercurrent flow of the hot gas. Finally, the solid is transferred to the lower end where it reaches the desired temperature and is discharged.

In the present study, the kiln can be divided into three sections. In the first section, the wet solids are heated to the boiling point of the entrained liquid. In the second section, the liquid evaporates at constant temperature until the feed is completely dry. In the third section, the solids are heated to some specified temperature and then are discharged from the kiln.

Figure 1(a) shows the nomenclature of the kiln. The angle, α, is called the fill-angle which shows the region of volume containing the solid. Figure 1(b) shows the heat transfer processes occurring in the kiln.

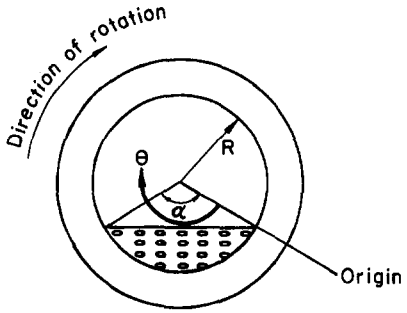

Fig. 1(a) Nomenclature of the kiln

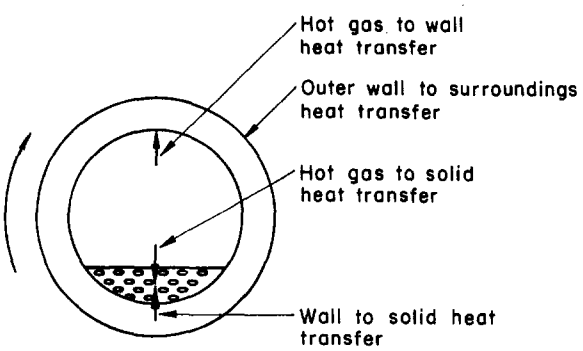

Fig. 1(b) Schematic diagram showing heat transfer processes in a rotary kiln

Associate Professor,[1] Former Graduate Student,[2] Department of Mechanical Engineering, Indian Institute of Technology, Kanpur, Kanpur, U.P. 208016, India.

An earlier version of this paper was presented at the 1989 ASME National Heat Transfer Conference, Philadelphia, August 6–9.

Contributed by the Manufacturing Division for publication in the JOURNAL OF ENGINEERING FOR INDUSTRY. Manuscript received May 1992; revised October 1994. Associate Technical Editor: A. Lavine.

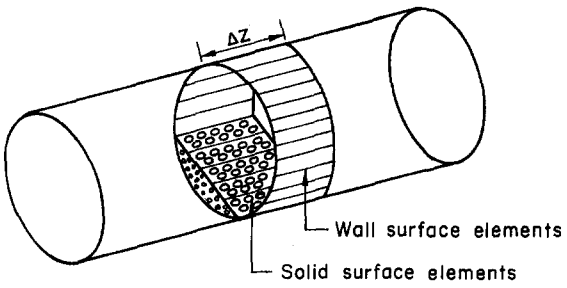

Fig. 2 Section of the kiln showing surface elements of the wall and the solid

Sass (1967) and Manitius et al. (1974) developed heat transfer models for a rotary kiln dryer and an aluminium oxide rotary kiln, respectively, using empirical relations for radiation exchange calculations. Manson and Unger (1979) described the heat transfer processes in a rotary kiln incinerator but did not perform a detailed analysis. Ghoshdastidar et al. (1985) developed a detailed steady-state heat transfer model for the rotary kiln waste incinerator burning plexiglas.

The present work differs from Sass (1967) by mainly two factors. First, the heat transfer modeling of the kiln is more rigorous and secondly, a detailed parametric study has been performed using this model.

2 Problem Formulation

2.1 Thermal Radiation Among Hot Gas, Refractory Wall and Solid Surface. Heat is exchanged among the hot gas, the inner wall of the kiln and the solid surface by radiation as the gas temperature is very high. The wall is divided into surface elements as shown in Fig. 2. Each axial segment (of size equal to 1 m) of the refractory surface is divided into fifteen surface elements of equal size. The solid surface is divided into five surface elements. The temperature of the solid surface element and the gas element are assumed to be uniform in each axial segment.

The surfaces are assumed diffuse and gray. It is assumed that the surface elements exchange radiation only with surfaces of the same axial segment.

The shape factors between two refractory surface elements and between one refractory surface element and one solid surface element are determined assuming the surfaces are infinite parallel strips (Jacob, 1957) as the axial temperature gradients are expected to be small. The net energy transfer, q_j, for a particular surface can be expressed as (Hottel, 1954):

$$q_j = \frac{\epsilon + 1}{2}\left[A_g F_{gj} \epsilon_g(T_g) E_{b_g} + \sum_{i=1}^{N} A_i F_{ij} \tau_g(T_i) E_{b_i} - E_{b_j} A_j\right] \quad (1)$$

where ϵ is the emissivity of the enclosure walls. Equation (1) is valid for $\epsilon > 0.8$. $\epsilon_g(T_g)$ and $\tau_g(T_i)$ indicate that the emissivity and the transmissivity of the gas are evaluated at T_g and T_i, respectively. Since the gas composition for this kiln is not given in Sass (1967), the composition (by volume) of hot gas mixture for a typical cement kiln is taken from Weber (1963) and is as follows: CO_2 - 15.89 percent, O_2 - 1.418 percent, N_2 - 41.784 percent, H_2O (vapor) - 40.9 percent. The pressure inside the kiln is assumed to be of one atmosphere. As CO_2, H_2O show band absorptance characteristics, the Mean Beam length theory of Hottel (Holman, 1981) is used to calculate gas emissivity and other characteristics.

2.2 Conduction Heat Transfer in the Refractory Wall. Since wall elements of the kiln are alternately heated and cooled during each revolution by the hot gas and the solid, respectively, quasi-steady heat conduction is present. Only heat conduction in the radial direction of the wall is taken into account, assuming negligible conduction in the circumferential and axial direction. A non-rotating coordinate system is used to model the wall heat conduction. Because the refractory thickness is small compared to the diameter, Cartesian coordinates are used.

Surface elements not covered by the solids are exposed to the radiation heat input, q_j's while those covered by the solids exchange heat with the solids primarily by surface contact. The contact heat transfer coefficient shown in Table 1 is an estimate obtained from Helmrich and Schügerl (1980). The boundary condition for the outer surface of the refractory wall is the heat loss by convection and radiation (Suryanarayana et al., 1986).

2.3 Energy Transport in the Solid. Mass and energy balances on an element of solid contained in an axial segment either in the first or in the third section of the kiln gives the expression for $T_{s,z+\Delta z}$ while the same performed on an element of the wet solids contained in an axial segment in the second section of the kiln gives the expression for the rate of evaporation, $\dot{m}_v$. It may be noted that the temperature of the solids in the second section remains constant at the saturation temperature of water. It is assumed that water is always available on the solid surface. The end of the second section is indicated where the cumulative $\dot{m}_v$ is equal to the total predetermined amount of water to be evaporated per second.

2.4 Energy Balance in the Gas. Mass and energy balances on an element of the hot gas contained in an axial segment in the first or third section of the kiln gives the expression for $T_{g,z+\Delta z}$ while the same performed on an element of the hot gas contained in an axial segment of the second section of the kiln gives another expression for $T_{g,z+\Delta z}$. In the second section, the superheating of the vapor is taken into account.

3 Method of Solution

A computer program is developed to obtain numerical results for the present problem. Input data are shown in Table 1. Finite

Table 1 Input data to the program

I Rotary kiln	
A Diameter	1.95 m
B Refractory	
1 Thickness	0.3 m
2 Thermal conductivity	1.3274 W/m-K
3 Specific heat	692.556 J/kg-K
4 Density	3000 kg/m^3
5 Emissivity	0.9
*C Rotational speed	1.87 rpm
*D Angle of inclination	2.53°
II Solid	
A Inlet temperature	366.66 K
B Outlet temperature	977.4 K
*C Mass flow rate (dry)	2.996 kg/sec
D Specific heat (average)	1122.54 J/kg-K
*E Water in solid feed	18% (by weight)
F Density	1500 kg/m^3
G Emissivity	0.95
III Gas	
*A Inlet temperature	1616.34 K
B Outlet temperaturre	935.77 K
C Specific heat (average)	1214.7 J/kg-K
*D Mass flow rate	5.9075 kg/sec.
IV Water	
A Latent heat of vaporization	2.26 × 10^6 J/kg
B Specific heat (vapor)	2083.2 J/kg K
C Specific heat (liquid)	4211.2 J/kg K
V Heat transfer coefficients	
A Contact heat transfer coefficient	64 W/m^2 K
B Convection heat transfer coefficient from the outer wall of the kiln to the surrounding	10 W/m^2 K
VI Ambient temperature outside the kiln	300 K
*VII Inlet fill-angle	90°

* Used only for comparison of the present results with those corresponding to the actual kiln.

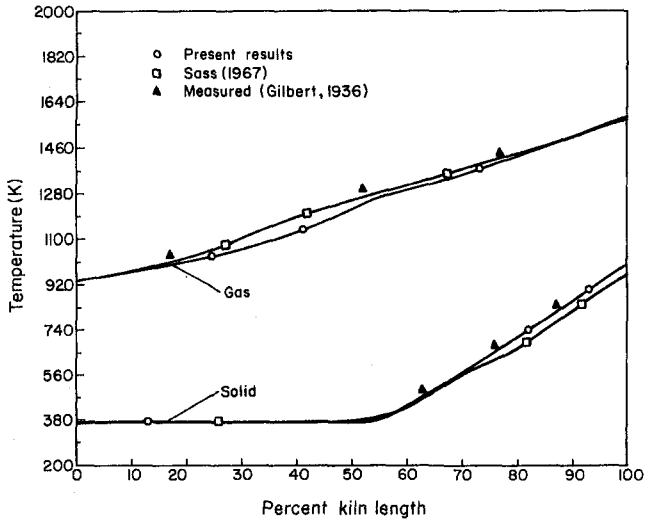

Fig. 3 Numerical and experimental axial temperature distributions of the solids and the gas based on the input data of Sass (1967)

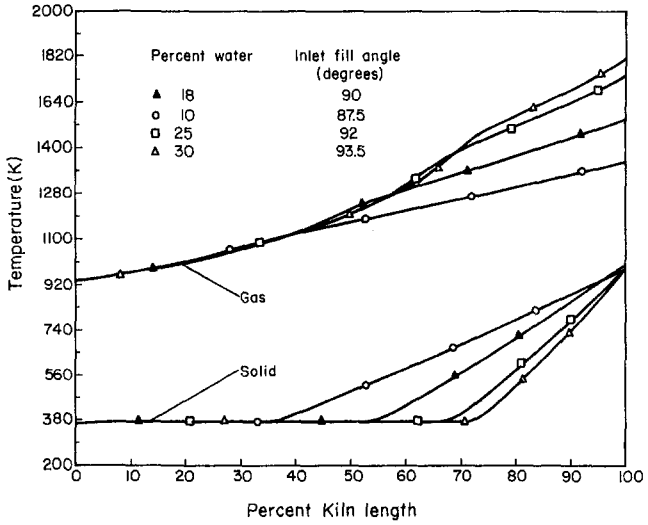

Fig. 4 Axial temperature distribution of the solids and the gas for various proportions of water in the solid feed

difference techniques are used and steady-state thermal conditions are assumed. A grid independence test has been done. False Transient approach is used to solve the wall conduction equation. The solution is initiated at the inlet of the kiln and proceeds to the exit. In the second section of the kiln, the change in shape factors due to removal of water from the solids is accounted for. The output data consists of refractory wall temperature, solids temperature, gas temperature, the individual lengths of the first, second and third section of the kiln and the total kiln length.

4 Results and Discussion

4.1 Validation With Earlier Experimental and Numerical Results. It is apparent from Fig. 3 that the simulation has accurately predicted the gas and solid temperature profile in the kiln, the fraction of the kiln used for water evaporation and the fraction used for heating the solids.

However, the kiln length predicted by the present model turns out to be 22 meters as compared to 25.5 meters predicted by Sass (1967), and 27.3 meters of the actual kiln. The deviation of the present predicted length from that of the actual kiln may be attributed to uncertainties in some of the input data such as the composition of the hot gas, contact heat transfer coefficient, the ambient temperature outside the kiln, the convective heat transfer coefficient from the kiln to the surrounding air, the speed of rotation of the kiln, the kiln inclination angle, the inlet fill-angle and the emissivity of the solid because the aforesaid data are not specified in Sass (1967) explicitly and therefore, are obtained in the present study either by using estimates or indirect calculations. Also, solid exit and gas-inlet temperature are based on estimates made by operating personnel as mentioned in Sass (1967).

4.2 Circumferential Temperature Variations. The results (figures not shown) also reveal that circumferential temperature variation in the kiln wall is very small.

4.3 Parametric Study

4.3.1 Axial Solid and Gas Temperature Distributions as Functions of Various Parameters. Figure 4 shows that with a higher percentage of water, in the third section of the kiln the axial gas temperature and dT_s/dz are higher while axial solid temperature with respect to percent kiln length is lower. This can be explained as follows. For a higher amount of water in the feed, the wet solid will have to traverse a greater distance to be completely dry. This means that although the same amount of dry solid will have to be heated to the same exit temperature and the fill angle remains the same in the third section no matter whether the solid contains more water or less, the total heat transfer to the solid in the last section of the kiln for the solid with a high water-content will be greater than that for a solid with a low water content, the reason being exposure of the dry solid to hotter gas in the former case as the heating starts closer to the outlet of the kiln which is the inlet for the hot gas. Therefore, to achieve the requisite exit temperature the dry solid will have to travel a smaller length of the kiln and hence dT_s/dz is higher while the axial solid temperature at the same percent kiln length is lower for the obvious reason.

Figure 5 shows that for higher solid mass flow rate, in the third section of the kiln the axial gas temperature is higher while the axial solid temperature is less. This can be explained by the fact that for larger solid mass flow rate the fill angle increases which in turn reduces mean beam length as the gas volume decreases and hence the emissivity of the gas decreases. This gives rise to lower loss of heat by the gas by radiation and hence the gas temperature is high. The solid temperature is less as the heat transfer by radiation to the solid is less and also

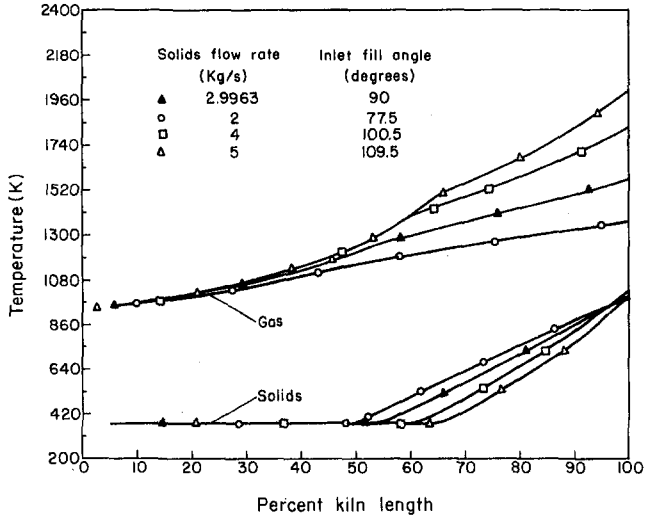

Fig. 5 Axial temperature distribution of the solids and the gas for different mass flow rates of the dry solids

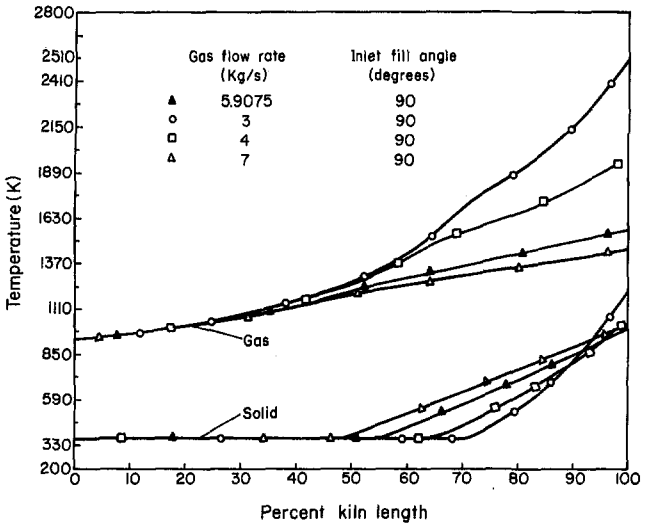

Fig. 6 Axial temperature distribution of the solids and the gas for different mass flow rates of the hot gas

because of the fact that for the case of higher solid mass flow rate, a greater amount of dry solids have to be heated.

Figure 6 shows that with higher gas flow rate the axial gas temperature is lower while the reverse is true for the axial solid temperature. This is because the higher gas flow rate implies that the gas residence time is less and hence the kiln has to be longer. This means the solid has to stay for a greater period of time in the kiln and therefore, solid temperature is high. The gas, on the other hand, loses more heat to the solids and hence the gas temperature is low. It is interesting to note the very high inlet gas temperature that is required for the lowest gas flow rate (3 kg/s). Using such hot inlet gas would be uneconomic although it would drastically reduce the kiln length.

It is also found (the graphs are not shown for the sake of brevity) that the axial gas temperature remains more or less independent of the angle of inclination (the present range, 2°–5°) of the kiln or rotational speed (the present range, 1–10 r.p.m.). This is expected as the gas flow is not a function of the aforesaid parameters. However, the axial solids temperature is greater for a higher angle of inclination of the kiln or for a higher rotational speed. Increase in the kiln inclination angle or the rotational speed increases the predicted kiln length and vice-versa.

5 Conclusions

A steady-state heat transfer model for a rotary kiln dryer with application to the nonreacting zone of a cement rotary kiln has been developed. The computer results show that the present model can predict the length of the kiln with reasonable accuracy. The deviation is due to uncertainties in some of the input data. The paper also presents a detailed parametric study which reveals that a good design of a rotary kiln requires medium gas flow rate, smaller angle of inclination and low rotational speed of the kiln.

References

1 Ghoshdastidar, P. S., Rhodes, C. A., and Orloff, D. I., 1985, "Heat Transfer in a Rotary Kiln during Incineration of Solid Waste," *23rd ASME National Heat Transfer Conference, Denver,* Colorado, August 4–7, ASME Paper No. 85–HT–86.

2 Gilbert, W., 1936, "Heat Transmission in Rotary Kilns," *Cement and Cement Manufacture,* Vol. 9, pp. 115–128, pp. 139–154, pp. 207–220.

3 Helmrich, H., and Schügerl, K., 1980, "Rotary Kiln Reactors in Chemical Industry," *Ger. Chem. Engg.,* Vol. 3, pp. 194–202.

4 Holman, J. P., 1981, *Heat Transfer.* pp. 341–348, 5th International Student Edition, McGraw Hill.

5 Hottel, H. C., 1954, "Heat Transmission," Chap. 4, *Radiant Heat Transmission,* W. H. McAdams, ed., 3rd ed., McGraw-Hill, New York.

6 Jacob, M., 1957, *Heat Transfer,* Vol. II, pp. 19–21, John Wiley & Sons, Inc., New York.

7 Manitius, A., Kureyuz, E., and Kawecki, W., 1974, "Mathematical Model of the Aluminium Oxide Rotary Kiln," *Ind. Eng. Chem. Process Design and Development,* Vol. 13, No. 2, pp. 132–142.

8 Manson, L., and Unger, S., 1979, "Hazardous Material Incineration Design Criteria," EPA Report No. 600/2-79-198, October.

9 Sass, A., 1967, "Simulation of the Heat Transfer Phenomena in a Rotary Kiln," *Ind. Eng. Chem. Process Design and Development,* Vol. 6, No. 4, pp. 532–535.

10 Suryanarayana, N. V., Lyon, J. E., and Kim, N. K., 1986, "Heat Shield for High Temperature Kiln," *Ind. Eng. Chem. Process Design and Development,* Vol. 25, pp. 843–849.

11 Weber, P., 1963, *Heat Transfer in Rotary Kilns,* Bauverlag Gmbh, Wiesbaden-Berlin.